https://doi.org/10.5194/acp-2019-1210
Preprint. Discussion started: 4 February 2020

Atmospheric Chemistry and Physics
Discussions

Bias in CMIP6 models compared to observed regional dimming and brightening trends (1961-2014)

Kine Onsum Moseid[1], Michael Schulz[1,2], Trude Storelvmo[2], Ingeborg Rian Julsrud[2,1], Dirk Olivié[1], Pierre Nabat[3], Martin Wild[4], Jason N. S. Cole[5], and Toshihiko Takemura[6]

[1]Norwegian Meteorological Institute, Oslo, Norway
[2]University of Oslo, Oslo, Norway
[3]CNRM, Université de Toulouse, Météo-France, CNRS, Toulouse, France
[4]ETHZ, Zurich, Switzerland
[5]Canadian Centre for Climate Modelling and Analysis, Environment Canada
[6]Kyushu University, Fukuoka, Japan

Correspondence: Kine Onsum Moseid (kristineom@met.no)

Abstract. Anthropogenic aerosol emissions have increased considerably over the last century, but climate effects and quantification of the emissions are highly uncertain as one goes back in time. This uncertainty is partly due to a lack of observations in the pre-satellite era, and previous studies show that Earth system models (ESMs) do not adequately represent surface energy fluxes over the historical era. We investigated global and regional aerosol effects over the time period 1961-2014 by looking at surface downwelling shortwave radiation (SDSR). We used observations from ground stations as well as multiple experiments from five ESMs participating in the Coupled Model Intercomparison Project Version 6 (CMIP6). Our results show that this subset of models reproduces the observed transient SDSR well in Europe, but poorly in China. The models do not reproduce the observed trend reversal in SDSR in China in the late 1980s, which is attributed to a change in the emission of sulfur dioxide in this region. The emissions of SO_2 show no sign of a trend reversal that could explain the observed SDSR evolution over China, and neither do other aerosols relevant to SDSR. The results from various aerosol emission perturbation experiments from DAMIP, RFMIP and AerChemMIP suggest that its likely, that aerosol effects are responsible for the dimming signal, although not its full amplitude. Simulated cloud cover changes in the different models are not correlated with observed changes over China. Therefore we suggest that the discrepancy between modeled and observed SDSR evolution is partly caused by erroneous aerosol and aerosol precursor emission inventories. This is an important finding as it may help interpreting whether ESMs reproduce the historical climate evolution for the right or wrong reason.

1 Introduction

Aerosol particles scatter and absorb radiation, thereby altering Earth's energy balance. Anthropogenic aerosol emissions have substantially increased over the last century, but the quantification of the effect has been characterized by large uncertainties. Earth system models (ESMs) are used to reproduce the climate evolution of the past 165 years, and sparse aerosol-related observations in the pre-satellite era play a dominant role in the uncertainty connected to these historical experiments. An improved understanding of the historical aerosol effect would increase the accuracy and credibility of ESMs future climate projections.

https://doi.org/10.5194/acp-2019-1210
Preprint. Discussion started: 4 February 2020

Atmospheric Chemistry and Physics Discussions

Surface downwelling shortwave radiation (SDSR) can serve as a proxy for aerosol effects, and the Global Energy Balance Archive (GEBA) dataset contains measurements of SDSR as far back as in 1922 (Wild et al., 2017). As such, it represents a unique and valuable data set for evaluation of simulated aerosol effects prior to the satellite era.

Observed SDSR reveals a widespread negative trend from the 1950s to the late 1980s, commonly referred to as “global dimming” (Liepert (2002), Wild (2016)). The magnitude of this dimming differs vastly between regions, as expected if the cause of dimming was in fact regionally varying increases in aerosol emissions, as has been proposed by Wild et al. (2007), Sanchez-Romero et al. (2014) and Wild (2016). In some areas a positive trend in SDSR follows the dimming, called "brightening". Previous studies show that historical simulations from ESMs do not reproduce the transient development of SDSR as observed (Storelvmo et al. (2018), Wild (2009)). The cause of this discrepancy is not known, but may be connected to uncertainties in aerosol emission inventories of the past, or, as Storelvmo et al. (2018) suggested, how models treat processes that translate aerosol emissions into radiative forcing.

Here we use the GEBA dataset together with several very recent CMIP6 historical model experiments from five ESMs to investigate the aerosol effect in the time period 1961-2014, globally and regionally. In the middle of this time period (around the late 1990s), the main region of high anthropogenic aerosol emissions shifted from Europe and North-America to Asia. We have chosen to focus on the regions of Europe and Asia in this study, as the models exhibit diverging abilities to reproduce the observed SDSR in these regions. We explore the relation between regional SDSR and aerosol emissions using a set of historical ESM experiments with differing aerosol emissions; some have pre-industrial aerosol emissions, while others use the most recent and best available historical aerosol emission inventory. (Hoesly et al., 2018). This paper thereby provides new insights into the question of whether state-of-the-art ESMs can adequately reproduce a part of the surface energy budget over the historical era. This is in turn an important indication of whether the ESMs reproduce the historical climate evolution for the right reason.

The paper is structured as follows: In Section 2 we begin by presenting the two observational datasets used, followed by a detailed description of the experiments simulated by the five models chosen to be part of this study. An explanation of the methods used to obtain and analyse the data complete Section 2. The results are presented in Section 3, starting with a global view of dimming and brightening before focusing on regional assessments of SDSR, clear sky SDSR, and cloud cover. Section 4 discusses the implications of our results and how they compare to previous studies, before final conclusions are presented in Section 5.

https://doi.org/10.5194/acp-2019-1210
Preprint. Discussion started: 4 February 2020

Atmospheric Chemistry and Physics Discussions

2 Data and Methods

2.1 Observations

The Global Energy Balance Archive (GEBA) holds data from ground-based stations measuring energy fluxes at the Earth's surface around the globe (Wild et al., 2017). Pyranometers were used in most of the measurement sites, which have an accuracy limitation of 3-5 % of the full signal (Michalsky et al. (1999), Wild et al. (2013)). We use the monthly mean data from 1487 stations in the time period 1961-2014 measuring downwelling shortwave radiation. The GEBA data set has been complemented by a machine learning technique (random forests (Breiman, 2001)) as in Storelvmo et al. (2018) to cover temporal gaps in the measurements and facilitate comparison to the gridded model data.

Monthly mean cloud cover data is taken from the Climate Research Unit Time Series 4.02 (CRU), which covers the period 1901-2017 (Harris et al., 2014). CRU consists of a climatology made from measurements at meteorological stations around the globe, interpolated to a 0.5^o latitude/longitude resolution grid covering continental areas.

2.2 Models and CMIP6

Five ESMs (NorESM2, CanESM5, MIROC6, CESM2 and CNRM-ESM2-1) were chosen for this study, based on available data and their involvement in relevant model intercomparison projects within the Coupled Model Intercomparison Project Phase 6 (CMIP6) (Eyring et al., 2016). As this study focuses on dimming and brightening, we have chosen experiments from model intercomparison projects (MIPs) that include perturbed historical simulations with which one can single out the effect of anthropogenic aerosol emissions on our diagnostic variables. An overview of models and experiments covering the proposed CMIP6 reference and perturbation studies can be found in Table 1. This section will give a more detailed description of the experiments in Table 1 and explain why they were chosen.

Every model that takes part in CMIP6 has to deliver a set of common experiments, among these the *historical* simulation. As can be seen in Table 1 this is the one experiment for which all the models have provided simulation results. All other experiments listed in Table 1 are simulations covering the historical period but with specific alterations dependent on what intercomparison project they are a part of.

The Detection and Attribution Model Intercomparison Project (DAMIP) has the goal of improving estimations of the climate response to individual forcings (Gillett et al., 2016) and includes three relevant experiments. The experiment tracing the impact of exclusively the anthropogenically emitted aerosols as forcing agents over the historical period, is called *hist-aer*. The *hist-nat* experiment consists of only the perturbation due to the evolution of the natural forcing, e.g. from stratospheric aerosols from volcanoes and solar irradiance variations. Finally, the *hist-GHG* experiment has only forcings from changes in the well mixed greenhouse gases. These experiments were chosen as they give a unique insight into how a fully coupled earth system model

https://doi.org/10.5194/acp-2019-1210
Preprint. Discussion started: 4 February 2020

attributes responses over the historical period to the different climate forcers.

While DAMIP provides a good framework for one of the main questions in CMIP6, namely how the Earth system responds to forcing, the RFMIP intercomparison focuses on understanding the forcing itself. The Radiative Forcing Model Intercomparison Project (RFMIP) contains a large set of experiments to further understand the radiative forcing of the past and the present (Pincus et al., 2016). We use two experiments from RFMIP, both with sea surface temperatures fixed to pre-industrial values. One experiment includes both anthropogenic and natural aerosol emissions (piClim-histall) while the other only includes anthropogenic emissions (piClim-histaer). When sea surface temperatures are kept to pre-industrial values the global surface temperature development stales, and one can say we have a pre-industrial climate. Sea surface temperatures can also have an effect on cloud cover, which in turn affect SDSR. So these experiments will show to what extent the removal of cloud cover change from global warming has an effect on SDSR. In addition, these RFMIP experiments are therefore useful to investigate how, or if, aerosol effects are dependent on global warming.

The third MIP included in this study is the Aerosol Chemistry Model Intercomparison Project (AerChemMIP), which is designed to answer questions regarding the effect aerosols and other near-term climate forcers (NTCF) can have on climate. NTCFs include methane, tropospheric ozone, aerosols and their precursors (Collins et al., 2017). Three experiments have been selected from AerChemMIP, two of which have pre-industrial aerosols emissions (hist-piAer) and pre-industrial NTCFs (hist-piNTCF), respectively, while the last experiment has prescribed sea surface temperatures from the historical simulation (histSST), with all forcing agents included. These experiments were chosen to see wether historical changes in tropospheric ozone, or wether a mixing layer in the ocean may have had an effect on dimming.

2.3 Methods

The GEBA stations have been divided into regions based on the country and continent each GEBA station is registered to. The number of stations in a region is presented together with the first results in Figure 1. All model output and CRU results have been co-located to GEBA station locations using the nearest neighbour method. A global mean is defined here as the mean of a variable across all GEBA station locations. A regional mean is a mean of a variable across the GEBA station locations registered to that same region in the GEBA data. Every station has been weighted equally. When a result is shown as an anomaly, as opposed to an absolute value, the general formula has been to subtract the mean of the first five years of the investigated time period (1961-2014) from the timeseries in question. These "baseline" values can be found in supplementary Table **??**.
The model data has been retrieved from The Earth System Grid Federation (ESGF) (Cinquini et al., 2014). ESGF is a data mangement system consisting of multiple geographically distributed nodes that coordinate through a peer-to-peer (P2P) protocol (Fan et al., 2015). We have used one ensemble member per experiment, as not every experiment had the option of providing more than one simulation. Since we are working with values that are highly variable a centered running mean of 10 years has been used as a smoothing technique.

https://doi.org/10.5194/acp-2019-1210
Preprint. Discussion started: 4 February 2020

3 Results

3.1 Dimming and brightening

The change in SDSR in the *historical* simulations from the five models is presented together with GEBA data in Figure 1. Model simulations show similar patterns of global SDSR to observations, but are remarkably different in magnitude.

To further identify from where these discrepancy originate, we consider the geographical regions separately. Asia and Europe are relevant regions in regards to anthropogenic aerosol emissions (as explained in Section 1) and thereby also relevant to global dimming and brightening. The historical SDSR evolution in Europe and Asia are presented in Figure 1 (b) and (c), respectively. European SDSR is relatively well represented by the model simulations, while the ground stations in Asia show a noticeable trend reversal in SDSR around the early 1990s that is not apparent in the model simulations. The historical model simulations show a consistent negative trend during the entire historical period in question in Asia. Historically, countries with relatively high emissions in Asia include India, Japan, and China (Hoesly et al., 2018), and the SDSR evolutions for each of these countries are shown in Figure 1 (d), (e), and (f), respectively. Figure 1 (d) shows that the models capture a relatively strong negative trend of SDSR in India, with MIROC6 being the model with the most modest trend. There are evident differences between observations and simulations in both Japan and China. Ground stations in Japan show a sharp decrease in SDSR until the early 1970s followed by some variations until a new minimum value is reached around 1990 before an increase in SDSR is measured. The minimum value around 1990 and the following positive trend is very similar to that of China, and Japan is believed to be heavily influenced by aerosol emissions from China from 1980 and onwards. Model simulations do not capture the magnitude of dimming in Japan but similar SDSR temporal tendencies can be identified in both observations and simulations.

Observations from China (Figure 1 (f)) show a trend reversal in SDSR similar to the one identified in Figure 1 (c) for Asia as a whole. In general the historical model simulations have similar end points as the observations in China and Asia as a whole. However, their temporal evolution does not show the observed trend reversal around the late 1980s in China, but rather a continuous negative trend throughout the period. This in turn suggests that the temporal forcing evolution of the last half century in the ESMs is not consistent with observations for Asia.

3.2 Dimming and brightening over China in various CMIP6 experiments

The CMIP6 framework consists of many simulations that can help investigate dimming and brightening (as explained in Section 2.2). In order to understand which forcing agents are responsible for the overall trends in SDSR in the models, we now investigate China for the experiments listed in Tabel 1. Figure 2 (a) shows the historical simulations together with observations of SDSR as previously seen in Figure 1 (f). Figure 2 (b), (c), and (d) shows the SDSR from experiments in DAMIP, RFMIP and AerChemMIP, respectively.

Out of the three experiments in DAMIP, only one of them contains the evolution of anthropogenic aerosol emissions, *hist-aer*, and this experiment clearly diverges from the other DAMIP experiments over time. SDSR from *hist-aer* shows patterns similar to the *historical* simulations, with start- and end-points comparable to the observations, but also still without the trend reversal seen in the observed temporal evolution of SDSR. SDSR in the experiments *hist-nat* and *hist-GHG* do not show signs of dimming or brightening over the investigated period.

In the RFMIP experiments, where both piClim-histaer and piClim-histall contain anthropogenic aerosol emissions, all simulations show a continuous dimming throughout the period, but like in the historical simulations there is no apparent trend reversal in the late 1980s. Two of the models (NorESM2 and CanESM5) exhibit a more negative SDSR when letting evolving aerosols impact the radiation alone, without GHGs. By comparing the historical with the piClim-histall experiments, one can also note that the choice of the coupling and sea surface temperatures do not seem to affect SDSR largely.

Out of the three experiments from AerChemMIP only histSST contains anthropogenic aerosol emissions. This is clear from how histSST simulations diverge from the other simulation as time progresses shown in Figure 2 (d). The simulations with pre-industrial aerosols (hist-piAer) and pre-industial near term climate forcers, including aerosols and ozone (hist-piNTCF) show very small or negligible changes in the SDSR over the time period considered.

Overall there is a clear difference in SDSR between experiments that include anthropogenic aerosol emissions and experiments that do not. Dimming is apparent in every simulation containing anthropogenic aerosol emissions, but absent in the simulations containing pre-industrial aerosols only. This points to anthropogenic aerosol emissions playing a key role in global dimming. Whether the sea surface temperature is pre-industrial, prescribed historical, or decided by a coupled ocean model seems to be unimportant for the SDSR in most models.
No trend reversal is identified in any of the simulations in which dimming is identified, and therefore none of the model simulations show a temporal evolution of SDSR close to the one seen in observations over China.

All-sky SDSR changes can be further decomposed into a clear-sky contribution as well as a contribution from changes in cloud cover and/or other cloud properties. In the next section we present the decomposed contributions to all-sky SDSR in China to further understand the discrepancy seen in Figure 2.

3.3 Clear sky SDSR and cloud cover in China

Clear-sky SDSR over China for the historical CMIP6 simulation is shown together with all-sky SDSR over China from GEBA in Figure 3 (a). If the simulated dimming is primarily caused by aerosol-radiation interactions, the dimming is stronger in the clear-sky SDSR for all models compared to the all-sky SDSR. This is exactly what we see in Figure 3 (a). All models and observation show a change in behaviour in the late 1990s until 2010, where models show a steepening of their dimming trend while the observations go from a brightening trend to a SDSR stabilisation. This can be related to the cloud cover change presented in Figure 3 (b), where all models except for MIROC6 show a decrease in cloud cover over the same period. A decrease in cloud cover would entail a brightening, and will therefore act as a mask for the steep decrease in clear sky SDSR. The simulated

https://doi.org/10.5194/acp-2019-1210
Preprint. Discussion started: 4 February 2020

cloud cover changes are presented together with cloud cover observations from CRU in Figure 3 (b). The transient change in cloud cover presented by CRU are, if anything, opposite of what they would have to be to explain the observed All-sky SDSR. It is important to note that the robustness of observed cloud cover changes must be verified by satellite observations, which goes beyond the scope of this study.

The pronounced trend reversal in observed all sky SDSR in the late 1980s in China is neither identified in all sky SDSR, clear sky SDSR, nor cloud cover in any of the model simulations.

In section 3.2, we showed that a dimming was only apparent in simulations that included anthropogenic aerosol emissions. In this session we found the clear-sky SDSR to be stronger than all-sky SDSR, indicating the simulated dimming is primarily caused by aerosol-radiation interactions. The next section will then show how the simulated aerosol burdens are connected to SDSR.

3.4 Atmospheric burden of SO_4

In the atmosphere, the actual *presence* of an aerosol is of course what scatters shortwave radiation, and the emissions of its precursor is only an indirect indicator of this presence. Therefore, we present the simulated change in burden of SO_4 over Europe, a location where dimming and brightening was well represented in simulations, and over China, where dimming and brightening was poorly represented in simulations (Figure 4 (a) and (b) respectively). As expected if sulfate aerosols have in fact played an important role in European dimming and brightening, the simulated burden of SO_4 shows a strikingly similar pattern (but with opposite sign) as the observed SDSR over Europe for all models. The maximum burden is found in the early to mid 1980s depending on the model, and the minimum SDSR around the same time. The various models differ in the magnitude of change in SO_4 burden over Europe but all show similar tendencies. NorESM2 is the model with the largest changes, and CESM2 is the model with the smallest changes in SO_2 burden. The same is observed over China, where NorESM2 has double the SO_4 burden at the end of the time period than the next model. In contrast to Europe, the observed SDSR does not mirror well to the simulated SO_4 burden over the GEBA stations in China. In order for the SO_4 burden to be the main cause of the observed changes in SDSR, the Asian SO_4 burden would have to peak around the late 1980s, which is not seen in the models in Figure 4 (b). All the simulated historical SO_4 burdens increase until 2010, showing no signs of the trend reversal identified in the GEBA data. Assuming GEBA data shows the real story, the problem in SO_4 burden must come from either the emissions or in the removal processes of SO_4.

Figure 5 shows emitted sulfur dioxide over China, the precursor of SO_2, for four of the models in this study. Emission sources are not expected to be at the same locations as GEBA stations, so the results shown Figure 5 is for a defined area as stated in the figure caption. Recall we are looking for signs of the observed trend reversal present in GEBA in Figure 4 (b) around the late 1980s. Figure 5 displays no trend reversal in SO_2 emissions between 1980 and 1990. The simulated burden of SO_4 co-located to GEBA stations in China presents a similar behaviour as the emitted SO_2 over China. Therefore the temporal development of SDSR seen in GEBA cannot be expected from the current emission inventories, given sulfate play an important part in SDSR in China.

https://doi.org/10.5194/acp-2019-1210
Preprint. Discussion started: 4 February 2020

Aerosol emissions in China and Asia as a whole has increased greatly over the last century. This includes more than just sulfur dioxide. Especially black carbon (BC) and organic carbon (OC) has had a strong increase in emissions in China. In the next section we will consider these aerosols and their potential influence on SDSR, together with a general discussion on our results.

4 Discussion

The climate effect of aerosol emissions over the industrial era is poorly constrained, in part due to lack of observations and uncertainty in emissions. The uncertainty in aerosol climate effects of the past is an important reason for the large spread in climate projections for the future. GEBA provides valuable observations of historical shortwave radiation at the surface that are of great value for model evaluation.

We have shown that a subset of models participating in CMIP6 do not accurately represent the observed dimming and brightening trends globally and regionally in their *historical* simulation. This is comparable to that of Storelvmo et al. (2018), who showed that the CMIP5 ensemble mean SDSR globally co-located to GEBA stations does not represent dimming or brightening. Our findings show that reproducibility of SDSR have not improved from CMIP5 to CMIP6. We find that while most models have similar change in SDSR as observations in the most recent years, the development over time greatly differs between model and observations, especially in China. This is in agreement with Allen et al. (2013) who studied the CMIP5 ensemble mean and found a continuous dimming trend over China, but with a severely underestimated magnitude of modelled clear-sky SDSR during the dimming period compared to a clear-sky proxy based on GEBA data.
China stands out as a region of interest as the observed SDSR shows a trend reversal in the mid 1980s that is not reproduced in the *historical* simulation by any of the models of this study.
The RFMIP experiments shown in Figure 2 displayed that sea surface temperatures did not noticeably affect SDSR on decadal timescales over China. This complements the findings by Folini and Wild (2015) where sea surface temperatures correlate to cloud cover, not aerosol effects.

Out of all the experiments presented in Table 1 and Figure 2, only those containing anthropogenic aerosol emissions showed dimming in China. This is expected as aerosols have been presented as the main cause of reduction in SDSR in China by previous studies (Wild, 2009; Yunfeng et al., 2001; Kaiser and Qian, 2002).
Storelvmo et al. (2018) argues that the discrepancy between observed and modelled SDSR can be attained to errors in the treatment of processes that translate aerosol emissions into clear-sky and all-sky radiative forcings. Here, we show that simulated SDSR develops similarly in time, but opposite in sign, to simulated atmospheric burden of SO_2. By doing this we narrow down the potential source of error by suggesting that the atmospheric burden in the models are at fault, and that the processes translating burden into clear-sky and all-sky radiative forcings are behaving as expected.
Atmospheric burdens are a result of emissions, gas-to-particle conversion, and wet-removal. The models of this study do a fairly good job in representing SDSR in Europe, so we assume both emissions and subsequent processes are well represented here.

https://doi.org/10.5194/acp-2019-1210
Preprint. Discussion started: 4 February 2020

The temporal development of SDSR is represented poorly in Asia, and specifically in China. Following the above logic this discrepancy could be rooted in errors in emissions or removal processes. The modeled emissions of SO_2 over China showed no trace of the trend reversal in observed SDSR between 1980 and 1990. Assuming sulfate burden is responsible for the observed trend reversal, we argue that errors in emissions inventories in China could be part of the problem. The sulfur dioxide emission inventory used as input for historical model simulations in CMIP6 is shown in Figure 3 corresponding to Hoesly et al. (2018). This figure also shows emission inventories of black carbon and organic carbon in China, and a closer look shows that neither of these aerosol emissions show tendencies matching a trend reversal in observed SDSR between 1980 and 1990.

Hoesly et al. (2018) have pointed to the need to study in the future emission uncertainties. Aas et al. (2019) have studied global and regional trends in atmospheric sulfur and found that uncertainties in emissions was largest in Asia, even though their study only went back to 1990.

5 Conclusions

An earlier study has shown that previous generations of Earth System Models have not been able to reproduce the transient development of surface downwelling shortwave radiation (SDSR) in the last decades since 1960 when observations became available. This discrepancy is hypothesized to be related to increasing and then partially decreasing trends in global aerosol emissions and subsequent aerosol radiative effects, but the exact cause is unknown.

In this paper, we compare observations to model simulated surface downwelling shortwave radiation and cloud cover in specific regions for the time period 1961 to 2014. We found that in the *historical* CMIP6 experiment models reproduce the transient development of SDSR well in Europe, but poorly in Asia. Observations in Asia exhibit a trend reversal in SDSR in the late 1980s that is primarily driven by SDSR changes in China. The multiple historical and historical perturbation experiments performed under CMIP6 reveal, that, in China, only those simulations containing anthropogenic aerosol emissions show dimming. None of the simulations exhibit the observed trend reversal over China in the late 1980s (brightening). We suggest that the continuous decrease in SDSR is related to the continuous increase in atmospheric sulfate burden in the *historical* simulations over China. Following this logic, the observed transient development of SDSR points to the sulfate burden in the models being wrong in this region. The sulfate burden is a result of sulfur dioxide emissions, gas-to-particle conversion and wet deposition. sulfur dioxide emissions over China show no sign of the observed trend reversal in SDSR and neither does black carbon nor organic carbon emissions. We suggest that the cause of the discrepancy between model and observations in transient SDSR in China is partly in erroneous emission inventories.

As the observed climate change is the result of warming from greenhouse gases and simultaneous cooling from aerosol radiative effects, getting aerosol emissions correct is an important part in earth system models ability to simulate the past for the right reasons.

https://doi.org/10.5194/acp-2019-1210
Preprint. Discussion started: 4 February 2020

Further studies could include other observations and proxies for aerosol effects in the historical era, such as long-term satellite retrieved aerosol optical depth, deposition of anthropogenic sulphur, organic carbon and nitrate in ice cores, as well as daily temperature range records.

https://doi.org/10.5194/acp-2019-1210
Preprint. Discussion started: 4 February 2020

Atmospheric Chemistry and Physics Discussions
Open Access
EGU

Table 1. Model participation, as used in this study, in CMIP6 model intercomparison projects (MIP) and their experiments.

MIP	Experiment	NorESM2	CanESM5	MIROC6	CESM2	CNRM-ESM2-1	Forcing agents
CMIP6	historical	x	x	x	x	x	All
DAMIP	hist-aer	x	x	x			Anthr. Aer
	hist-GHG	x	x	x			Anthr. GHG
	hist-nat	x	x		x		Volc. and solar
RFMIP	piClim-histaer	x	x	x			Anthr. Aer
	piClim-histall	x	x	x			All
AerChemMIP	hist-piAer	x		x			Volc.,solar,GHG
	hist-piNTCF	x		x		x	Volc.,solar,GHG
	histSST	x		x		x	All

https://doi.org/10.5194/acp-2019-1210
Preprint. Discussion started: 4 February 2020

Atmospheric Chemistry and Physics Discussions

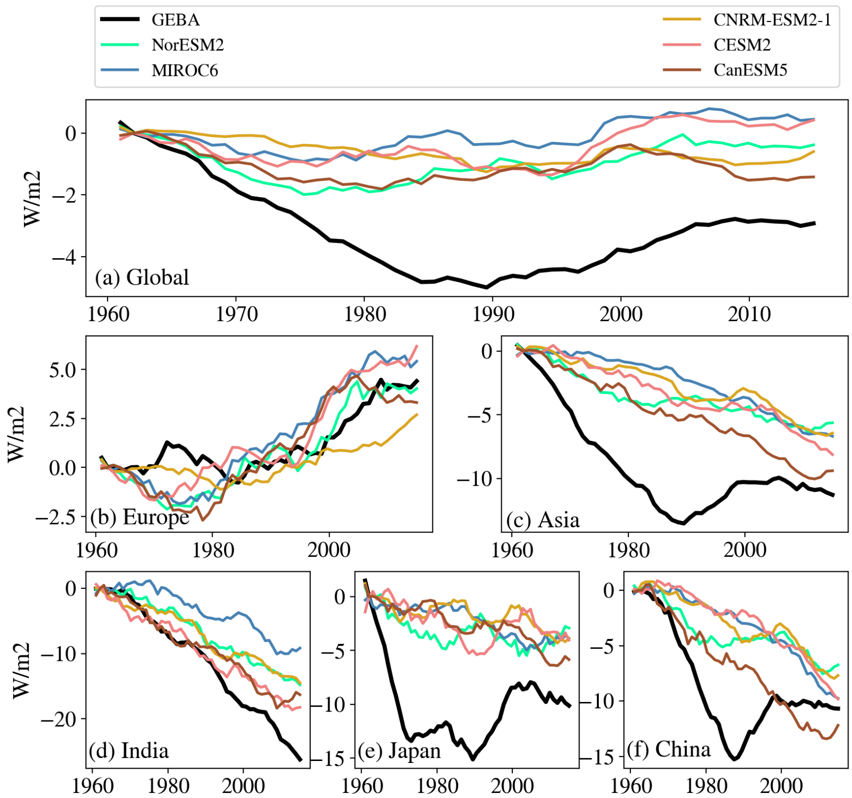

Figure 1. Surface downwelling shortwave radiation (SDSR) anomaly at the surface for GEBA and five earth system models. Results are co-located at (a) all GEBA stations (1487), (b) European (503), (c) Asian (311), (d), Indian (15), (e) Japanese (100), and (f) Chinese (119) stations. Numbers in parenthesis are number of ground stations in respective region.

https://doi.org/10.5194/acp-2019-1210
Preprint. Discussion started: 4 February 2020

Atmospheric Chemistry and Physics
Discussions

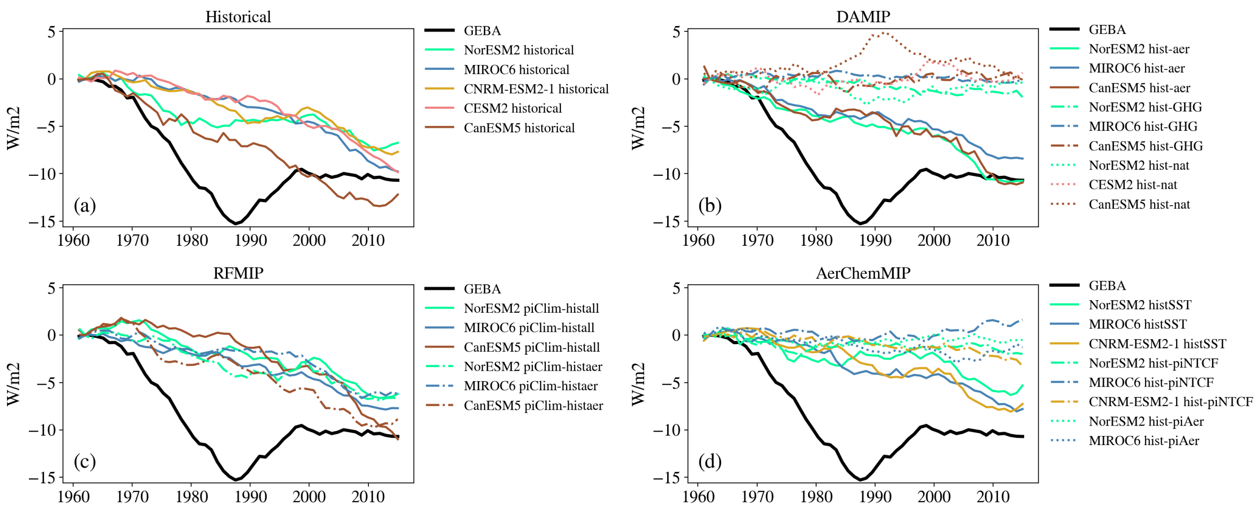

Figure 2. SDSR anomaly in China for all the CMIP6 simulations as listed in Table 1. All model results are co-located at GEBA station locations registered to China.

https://doi.org/10.5194/acp-2019-1210
Preprint. Discussion started: 4 February 2020

Atmospheric Chemistry and Physics
Discussions

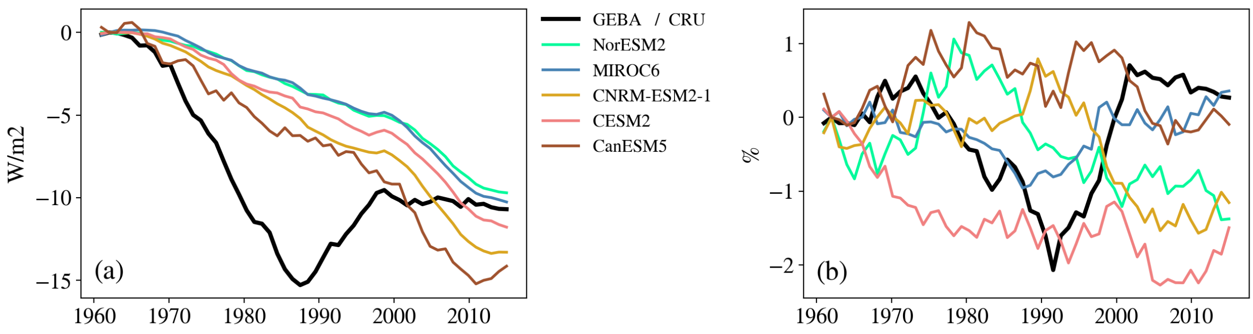

Figure 3. SDSR and cloud analysis at Chinese GEBA stations in historical experiments: a) Clear sky SDSR anomaly together with all sky GEBA SDSR anomaly and (b) cloud cover anomaly together with corresponding CRU data.

https://doi.org/10.5194/acp-2019-1210
Preprint. Discussion started: 4 February 2020

Atmospheric Chemistry and Physics
Discussions

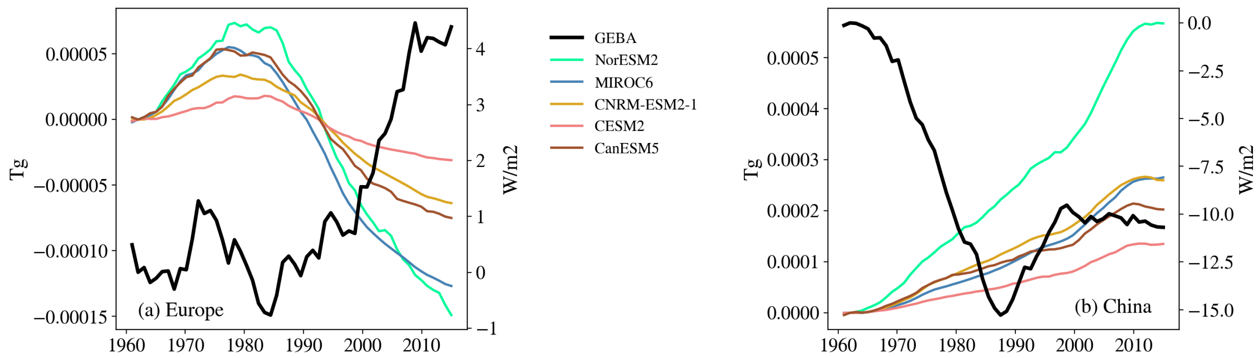

Figure 4. Anomaly of atmospheric load of sulfate together with observed all sky SDSR anomaly in (a) Europe and (b) China

.

https://doi.org/10.5194/acp-2019-1210
Preprint. Discussion started: 4 February 2020

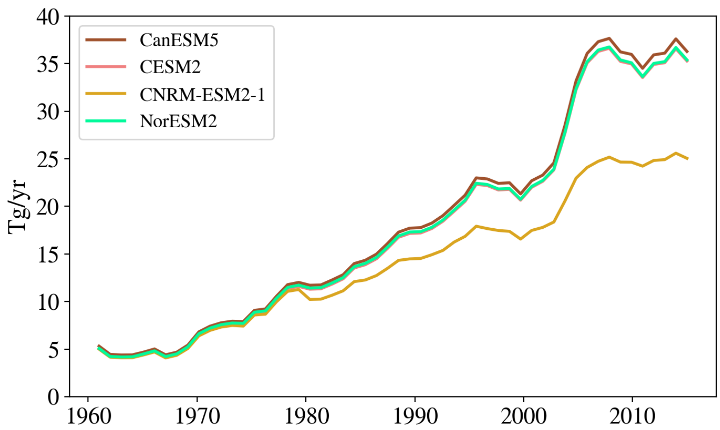

Figure 5. Emission of SO_2 in China, diagnosed by four of the models in this study. China is defined here as the area within latitudes [20°N–45°N], and longitudes [95°E–125°E].

https://doi.org/10.5194/acp-2019-1210
Preprint. Discussion started: 4 February 2020

Atmospheric Chemistry and Physics Discussions

Appendix A: tables

Table A1. SDSR and cloud cover averaged over the years 1961-1966 as observed (GEBA for radiation, CRU for cloud cover) and as simulated in the historical experiment by each of the models of this study. Data are retrieved after co-location at GEBA sites.

	Observation	NorESM2	CanESM5	MIROC6	CESM2	CNRM-EMS2-1
SDSR $[\mathrm{W/m^2}]$	176.7	187.6	189.7	184.3	186.3	192.4
Cloud Cover [%]	58.5	55.3	56.0	50.3	63.8	57.3

Author contributions. KM wrote most of the article and did all analysis of CMIP6 data. MS and TS contributed to design of the study and helped editing the text. DO, PN, JC and TT contributed model data via the ESGF CMIP6 archive. IJ and MW contributed with observational data. All co-authors contributed to the analysis and gave feedback to the manuscript.

Competing interests. No competing interests

Acknowledgements. This study benefited greatly from the CMIP6 data infrastructure for handling and providing model data for analysis. KM, MS and TS acknowledge funding from the European Union's Horizon 2020 project FORCeS under grant agreement No 821205. We acknowledge support from the Research Council of Norway funded project KeyClim (295046). Jan Griesfeller is thanked for data organisation. High performance computing and storage resources were provided by the Norwegian infrastructure for computational science (through projects NS2345K, NS9560K and NS9252K) and the Norwegian Meteorological Institute. TT was supported by the supercomputer system of the National Institute for Environmental Studies, Japan, and JSPS KAKENHI Grant Number JP19H05669.

https://doi.org/10.5194/acp-2019-1210
Preprint. Discussion started: 4 February 2020

References

Aas, W., Mortier, A., Bowersox, V., Cherian, R., Faluvegi, G., Fagerli, H., Hand, J., Klimont, Z., Galy-Lacaux, C., Lehmann, C. M. B., Myhre, C. L., Myhre, G., Olivié, D., Sato, K., Quaas, J., Rao, P. S. P., Schulz, M., Shindell, D., Skeie, R. B., Stein, A., Takemura, T., Tsyro, S., Vet, R., and Xu, X.: Global and regional trends of atmospheric sulfur, Scientific Reports, 9, 953, https://doi.org/10.1038/s41598-018-37304-0, https://www.nature.com/articles/s41598-018-37304-0, 2019.

Allen, R. J., Norris, J. R., and Wild, M.: Evaluation of multidecadal variability in CMIP5 surface solar radiation and inferred underestimation of aerosol direct effects over Europe, China, Japan, and India, Journal of Geophysical Research: Atmospheres, 118, 6311–6336, https://doi.org/10.1002/jgrd.50426, https://agupubs.onlinelibrary.wiley.com/doi/abs/10.1002/jgrd.50426, 2013.

Breiman, L.: Random Forests, Machine Learning, 45, 5–32, https://doi.org/10.1023/A:1010933404324, https://doi.org/10.1023/A:1010933404324, 2001.

Cinquini, L., Crichton, D., Mattmann, C., Harney, J., Shipman, G., Wang, F., Ananthakrishnan, R., Miller, N., Denvil, S., Morgan, M., Pobre, Z., Bell, G. M., Doutriaux, C., Drach, R., Williams, D., Kershaw, P., Pascoe, S., Gonzalez, E., Fiore, S., and Schweitzer, R.: The Earth System Grid Federation: An open infrastructure for access to distributed geospatial data, Future Generation Computer Systems, 36, 400–417, https://doi.org/10.1016/j.future.2013.07.002, http://www.sciencedirect.com/science/article/pii/S0167739X13001477, 2014.

Collins, W. J., Lamarque, J.-F., Schulz, M., Boucher, O., Eyring, V., Hegglin, M. I., Maycock, A., Myhre, G., Prather, M., Shindell, D., and Smith, S. J.: AerChemMIP: quantifying the effects of chemistry and aerosols in CMIP6, Geoscientific Model Development, 10, 585–607, https://doi.org/10.5194/gmd-10-585-2017, https://www.geosci-model-dev.net/10/585/2017/, 2017.

Eyring, V., Bony, S., Meehl, G. A., Senior, C. A., Stevens, B., Stouffer, R. J., and Taylor, K. E.: Overview of the Coupled Model Intercomparison Project Phase 6 (CMIP6) experimental design and organization, Geoscientific Model Development, 9, 1937–1958, https://doi.org/https://doi.org/10.5194/gmd-9-1937-2016, https://www.geosci-model-dev.net/9/1937/2016/gmd-9-1937-2016.html, 2016.

Fan, C., Shannigrahi, S., DiBenedetto, S., Olschanowsky, C., Papadopoulos, C., and Newman, H.: Managing Scientific Data with Named Data Networking, in: Proceedings of the Fifth International Workshop on Network-Aware Data Management, NDM '15, pp. 1:1–1:7, ACM, New York, NY, USA, https://doi.org/10.1145/2832099.2832100, http://doi.acm.org/10.1145/2832099.2832100, event-place: Austin, Texas, 2015.

Folini, D. and Wild, M.: The effect of aerosols and sea surface temperature on China's climate in the late twentieth century from ensembles of global climate simulations, Journal of Geophysical Research: Atmospheres, 120, 2261–2279, https://doi.org/10.1002/2014JD022851, https://agupubs.onlinelibrary.wiley.com/doi/abs/10.1002/2014JD022851, 2015.

Gillett, N. P., Shiogama, H., Funke, B., Hegerl, G., Knutti, R., Matthes, K., Santer, B. D., Stone, D., and Tebaldi, C.: The Detection and Attribution Model Intercomparison Project (DAMIP v1.0) contribution to CMIP6, Geoscientific Model Development, 9, 3685–3697, https://doi.org/https://doi.org/10.5194/gmd-9-3685-2016, https://www.geosci-model-dev.net/9/3685/2016/, 2016.

Harris, I., Jones, P. D., Osborn, T. J., and Lister, D. H.: Updated high-resolution grids of monthly climatic observations – the CRU TS3.10 Dataset, International Journal of Climatology, 34, 623–642, https://doi.org/10.1002/joc.3711, https://rmets.onlinelibrary.wiley.com/doi/abs/10.1002/joc.3711, 2014.

Hoesly, R. M., Smith, S. J., Feng, L., Klimont, Z., Janssens-Maenhout, G., Pitkanen, T., Seibert, J. J., Vu, L., Andres, R. J., Bolt, R. M., Bond, T. C., Dawidowski, L., Kholod, N., Kurokawa, J.-i., Li, M., Liu, L., Lu, Z., Moura, M. C. P., O'Rourke, P. R., and Zhang, Q.: Historical (1750–2014) anthropogenic emissions of reactive gases and aerosols from the Community Emissions Data System (CEDS), Geoscientific

https://doi.org/10.5194/acp-2019-1210
Preprint. Discussion started: 4 February 2020

Atmospheric Chemistry and Physics
Open Access
Discussions

Model Development, 11, 369–408, https://doi.org/https://doi.org/10.5194/gmd-11-369-2018, https://www.geosci-model-dev.net/11/369/2018/, 2018.

Kaiser, D. P. and Qian, Y.: Decreasing trends in sunshine duration over China for 1954–1998: Indication of increased haze pollution?, Geophysical Research Letters, 29, 38–1–38–4, https://doi.org/10.1029/2002GL016057, https://agupubs.onlinelibrary.wiley.com/doi/abs/10.1029/2002GL016057, 2002.

Liepert, B. G.: Observed reductions of surface solar radiation at sites in the United States and worldwide from 1961 to 1990, Geophysical Research Letters, 29, 61–1–61–4, https://doi.org/10.1029/2002GL014910, https://agupubs.onlinelibrary.wiley.com/doi/abs/10.1029/2002GL014910, 2002.

Michalsky, J., Dutton, E., Rubes, M., Nelson, D., Stoffel, T., Wesley, M., Splitt, M., and DeLuisi, J.: Optimal Measurement of Surface Shortwave Irradiance Using Current Instrumentation, Journal of Atmospheric and Oceanic Technology, 16, 55–69, https://doi.org/10.1175/1520-0426(1999)016<0055:OMOSSI>2.0.CO;2, https://journals.ametsoc.org/doi/full/10.1175/1520-0426%281999%29016%3C0055%3AOMOSSI%3E2.0.CO%3B2, 1999.

Pincus, R., Forster, P. M., and Stevens, B.: The Radiative Forcing Model Intercomparison Project (RFMIP): experimental protocol for CMIP6, Geoscientific Model Development, 9, 3447–3460, https://doi.org/https://doi.org/10.5194/gmd-9-3447-2016, https://www.geosci-model-dev.net/9/3447/2016/, 2016.

Sanchez-Romero, A., Sanchez-Lorenzo, A., Calbó, J., González, J. A., and Azorin-Molina, C.: The signal of aerosol-induced changes in sunshine duration records: A review of the evidence, Journal of Geophysical Research: Atmospheres, 119, 4657–4673, https://doi.org/10.1002/2013JD021393, https://agupubs.onlinelibrary.wiley.com/doi/abs/10.1002/2013JD021393, 2014.

Storelvmo, T., Heede, U. K., Leirvik, T., Phillips, P. C. B., Arndt, P., and Wild, M.: Lethargic Response to Aerosol Emissions in Current Climate Models, Geophysical Research Letters, 0, https://doi.org/10.1029/2018GL078298, https://agupubs.onlinelibrary.wiley.com/doi/abs/10.1029/2018GL078298, 2018.

Wild, M.: Global dimming and brightening: A review, Journal of Geophysical Research, 114, https://doi.org/10.1029/2008JD011470, http://doi.wiley.com/10.1029/2008JD011470, 2009.

Wild, M.: Decadal changes in radiative fluxes at land and ocean surfaces and their relevance for global warming, Wiley Interdisciplinary Reviews: Climate Change, 7, 91–107, https://doi.org/10.1002/wcc.372, https://onlinelibrary.wiley.com/doi/abs/10.1002/wcc.372, 2016.

Wild, M., Ohmura, A., and Makowski, K.: Impact of global dimming and brightening on global warming, Geophysical Research Letters, 34, https://doi.org/10.1029/2006GL028031, https://agupubs.onlinelibrary.wiley.com/doi/abs/10.1029/2006GL028031, 2007.

Wild, M., Folini, D., Schär, C., Loeb, N., Dutton, E. G., and König-Langlo, G.: The global energy balance from a surface perspective, Climate Dynamics, 40, 3107–3134, https://doi.org/10.1007/s00382-012-1569-8, https://doi.org/10.1007/s00382-012-1569-8, 2013.

Wild, M., Ohmura, A., Schär, C., Müller, G., Folini, D., Schwarz, M., Hakuba, M. Z., and Sanchez-Lorenzo, A.: The Global Energy Balance Archive (GEBA) version 2017: a database for worldwide measured surface energy fluxes, Earth System Science Data, 9, 601–613, https://doi.org/https://doi.org/10.5194/essd-9-601-2017, https://www.earth-syst-sci-data.net/9/601/2017/, 2017.

Yunfeng, L., Daren, L., Xiuji, Z., Weiliang, L., and Qing, H.: Characteristics of the spatial distribution and yearly variation of aerosol optical depth over China in last 30 years, Journal of Geophysical Research: Atmospheres, 106, 14 501–14 513, https://doi.org/10.1029/2001JD900030, https://agupubs.onlinelibrary.wiley.com/doi/abs/10.1029/2001JD900030, 2001.